Design analysis of a lead-lithium/supercritical CO_2 printed circuit heat exchanger for primary power recovery

Iván Fernández, Luis Sedano

EURATOM-CIEMAT Association, Av. Complutense, 40. 28040 Madrid (Spain)

One of the key issues for fusion power plant technology is the efficient, reliable and safe recovery of the power extracted by the primary coolants. An interesting design option for power conversion cycles based on Dual Coolant Breeding Blankets (DCBB) is a Printed Circuit Heat Exchanger, which is supported by the advantages of its compactness, thermal effectiveness, high temperature and pressure capability and corrosion resistance. This work presents a design analysis of a silicon carbide printed circuit heat exchanger for lead-lithium/supercritical CO_2 at DEMO ranges (4x segmentation).

Keywords: PCHE, SiC, airfoil, lithium-lead, supercritical CO_2.

1. Introduction

Tecno_Fus is a Spanish program to develop the dual-coolant breeding blanket design concept and its plant auxiliary systems for a future power reactor, which represents the best placed option in terms of power conversion efficiency. Recent results with eutectic lead-lithium as main primary nuclear power recovering fluid, and supercritical CO_2 for the secondary circuit, show gross efficiencies in the range of 47% in a recompression cycle (Feher cycle) coupled to a Rankine cycle [1].

Printed Circuit Heat Exchangers (PCHE) made up by diffusion-bonded thin plates with chemically etched channels, with semicircular cross section and zig-zag trajectories, begin to be widely used in experimental loops and the industry. The present work starts from these designs and explores the optimization of the printed circuit to minimize pressure drops with low penalization in heat transfer area by means of introducing airfoil shaped fins [2]. The issue of tritium permeation from primary to secondary coolant is also assessed. Computer fluid-dynamics and tritium transport tools have been used for these purposes, and the eutectic lead-lithium/supercritical CO_2 heat exchanger proposed in Tecno_Fus has been taken as the case of study.

2. Design of the PCHE

2.1 Structural material selection

Silicon carbide ceramics and SiC_f/SiC composites are among the most promising candidates as structural materials for fusion technology because of their potential application for high performance reactors and superior safety characteristics compared to metallic materials [3]. For DEMO DCLL blanket, thermal applications require heat and pressure resistances at high operating temperatures, compatibility with lead-lithium liquid metal breeder [4] and low tritium diffusivity and solubility. One important issue in this field is the development of SiC joining techniques, which include diffusion bonding using various active fillers, transient eutectic phase methods such as Nano-Infiltration and Transient Eutectic-phase (NITE), laser joining, selected area chemical vapor deposition, glass–ceramic joining, solid state displacement reactions and preceramic polymer routes [5]. NITE joining is believed to be the most promising option, since it is based on a joining zone having the same composition of NITE-SiC_f/SiC composites matrix. A scaled module of a NITE-SiC_f/SiC composite compact heat exchanger has been already built [6] and tested with notable performances from the point of view of heat transfer.

Silicon carbide is very resistant to chemical etching. However, chlorine-containing gas mixtures [7], hot potassium hydroxide (KOH) or reactive ion etching (RIE) are capable to etch the ceramic surface. They must be more developed, but they must be considered as candidate techniques to produce the printed circuit of the heat exchanger.

2.2 Geometric configuration

The characteristics of the power conversion cycle in Tecno_Fus program [1] determine several working parameters. Thus, PbLi and CO_2 mass flows ($\dot{m}_{PbLi} = 1.089 \cdot 10^4$ kg s-1, $\dot{m}_{CO2} = 2.875 \cdot 10^3$ kg s-1) and inlet temperatures ($T_{in\ PbLi}$ = 973 K, $T_{in\ CO2}$ = 664 K) are input data for the pre-sizing of the heat exchanger, as well as the inlet pressure for the CO_2 circuit (P_{CO2} = 200 bar).

author's email: ivan.fernandez@ciemat.es

The body of the PCHE is composed of a stack of plates which alternatively contain hot (PbLi) and cold (CO_2) streams. The arrangement of the streams is in counterflow. The inlet and the outlet of the cold fluid occurs at the opposite faces of the longer sides of the plates, due to the space needs of the manifolds, so two zones of cross-flow are needed. However, for the purposes of this work, we consider counterflow arrangement along the whole length of the heat exchanger.

The dimensions of each plate are 820 mm (length) x 588 mm (width) x 1.5 mm (thickness). Each plate contains airfoil shaped fins with 1.5 mm of height, whereas the end faces of the plates include a ledge to stiffen the joint between consecutive plates. The total number of plates for each fluid is 6000, which can be arranged in 10 modules of 1200 plates (total).

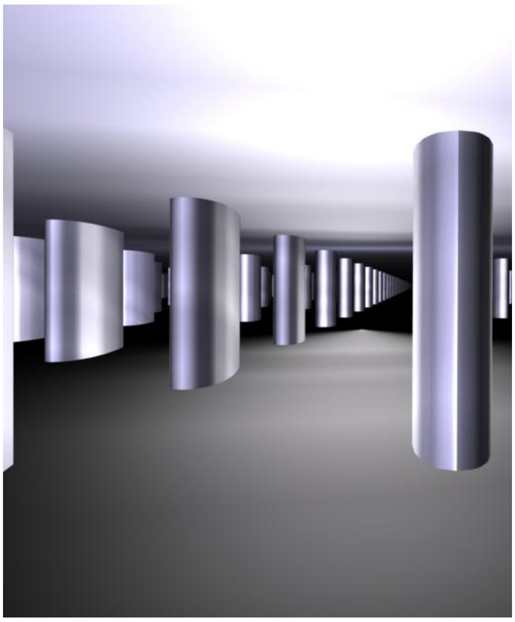

Figure 1. Rendered view of the interior of a channel.

2.2 Airfoils shape

The shape of the airfoil has been optimized to obtain a minimum resistance to the flown, by minimizing the drag coefficient (C_d) of the airfoil. NACA-4-digit series for aircraft wings, developed by the National Advisory Committee for Aeronautics (NACA), have been studied by using XFOIL, a code developed for the design and viscous (or inviscid) analysis of subsonic isolated airfoils. Given the coordinates specifying the shape of a 2D airfoil, angle of attack, Reynolds and Mach numbers, XFOIL can calculate the pressure distribution on the airfoil and hence lift and drag characteristics.

An interface code has been programmed in MATLAB to automatically execute XFOIL and analyze every NACA-4-digit profile with thickness of 10% of the chord, for a range of angle of attack of 0-4º, considering the Reynolds and Mach number estimated for the CO_2 stream, where is expected the larger pressure drop. The MATLAB code allows saving the profile name, the angle of attack and the values of C_d in a text file.

The profile with the smallest C_d for the given conditions is NACA 4110 with an angle of attack of 2.4º. However, this profile presents an asymmetry between their top and their bottom surfaces (camber), which is used to increase the lift coefficient of the airfoil in aeronautics. Since using a symmetric profile is preferable in our case, the selection is restricted to profiles with 0% of camber and 0º as angle of attack. Into this group, the NACA 0010 is the profile with smallest C_d.

3. 1-D heat transfer model

A one-dimensional heat transfer model has been used to pre-size the PCHE by evaluating the temperature profiles along the channels for both hot and cold streams [8].

The length of the PCHE is divided into a number of nodal segments. The temperature at a given node in each channel is considered as constant, as well as the specific heat, thermal conductivity, viscosity and density. The heat transferred from the hot side to each segment, q_n, can be expressed as:

$$q_n = \dot{m}_h \cdot Cp_h \cdot \left(T_{h_n} - T_{h_{n+1}}\right) \quad (1)$$

Where q, ṁ, Cp and T are the heat transfer rate, mass flow rate, specific heat and temperature, respectively. In a similar way, the heat transferred to the cold side can be calculated as follows:

$$q_n = \dot{m}_c \cdot Cp_c \cdot \left(T_{c_n} - T_{c_{n+1}}\right) \quad (2)$$

The Log Mean Temperature Difference (LMTD) method is applied to each segment of the PCHE:

$$q_n = U \cdot \frac{A}{n} \cdot \frac{\left(T_{h_n} - T_{c_n}\right) - \left(T_{h_{n+1}} - T_{c_{n+1}}\right)}{\ln\left(\dfrac{T_{h_n} - T_{c_n}}{T_{h_{n+1}} - T_{c_{n+1}}}\right)} \quad (3)$$

Where U is the overall heat transfer coefficient, A is the heat transfer area and n is the number of nodes. So we have three equations for each segment of the PCHE and we can establish the following equalities: (1) = (2) = (3).

A MATLAB code has been created to write the nodal equations and numerically solve the non-linear system. A total number of 20 nodes have been used, but the result is practically invariant inside a close range of numbers of nodes.

The capability of this 1-D model to predict the temperature profiles strongly depends on the estimation of the overall heat transfer coefficient, U:

$$U = \frac{1}{\dfrac{1}{h_h} + \dfrac{t}{k} + \dfrac{1}{h_c}} \quad (4)$$

Where h, t and k refer to convection heat transfer coefficient, effective thickness of the wall and thermal conductivity of the wall material, respectively. The evaluation of the Nusselt numbers for the lead-lithium and the CO_2 streams reveals strong differences between empirical correlations. Several correlations for forced convection heat transfer in pipes proposed by Gnielinski, Dittus-Boelter, Wang-Peng and Kottowski have been assessed. The results obtained by using Wang-Peng for the carbon dioxide and Kottowski for the lead-lithium are the most similar to the 3-D CFD results. Wang and Peng correlation [8] is a modification of the well-known Ditus-Boelter correlation for rectangular channels:

$$Nu = 0.00805 \cdot \mathrm{Re}^{0.8} \cdot \mathrm{Pr}^{0.4} \quad (5)$$

Kottowski proposed a suitable correlation for heat transfer in liquid metal fully developed turbulent flow through pipes with various geometrical shapes [6]:

$$Nu = \frac{2}{3} \cdot Nu_{sm} + 0.025 \cdot \left(\mathrm{Re} \cdot \mathrm{Pr}\right)^{0.8} \quad (6)$$

Where Nu_{sm} is the Nusselt number for slug flow. A value of 8.00 has been recommended [6].

The 1-D and CFD results are compared in the section 3.2.

3. 3-D CFD model

3.1 Scaled model

Numerical analyses have been performed to optimize the airfoil fins arrangement in terms of pressure drop and integrated thermal flux by varying the distance between the airfoils along the flow direction [2]. 3-D scaled models have been designed in CATIA. A Visual Basic macro to minimize the number of points to be linked by splines has been used to create the geometry of the airfoils. The scaled CAD model is composed by three reduced-size plates: two cold and a central hot. The size of the model is 25 mm (length) x 14 mm (width) x 9 mm (height).

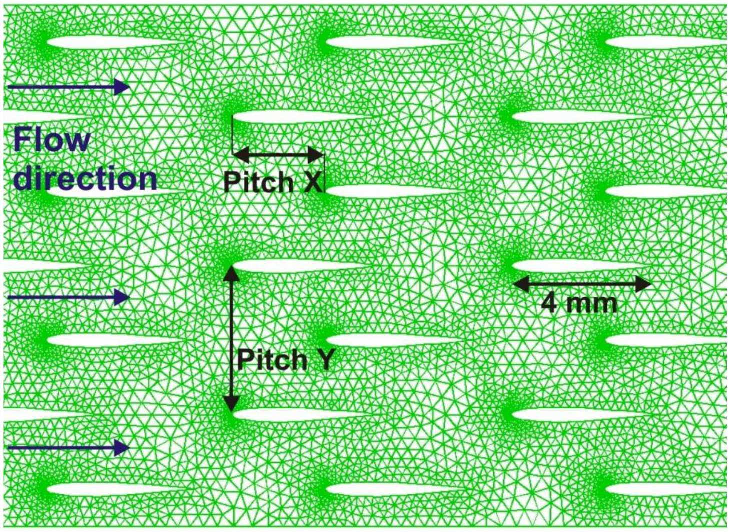

Figure 2. Channel configuration.

The steady-state fluid dynamics model with conjugated heat transfer has been defined and solved with ANSYS FLUENT. The size of the meshes was about 200,000 elements. The properties of the fluids have been maintained as constant [9] [10], since their variations in the considered ranges of temperature and pressure are not significant. For the thermal properties of silicon carbide, a low-porosity NITE-SiC has been taken as reference, due to its quite high thermal conductivity [11], although the SiC wall only exerts a small influence on the overall heat transfer coefficient.

Velocity-inlet and pressure-outlet have been established as boundary conditions for both streams, and the k-ε turbulence model has been used. The inlet temperatures mentioned in section 2.2 have been also introduced.

The results show that the minimum relation ΔP/Q occurs with the largest distance between airfoils. Both variables exhibit high values because the inlet velocities (v_{PbLi}=28 m/s; v_{CO2}=2 m/s) were calculated for a reduced number of plates (800):

Table 1: Results of the calculations.

Pitch X (mm)	Pich Y (mm)	ΔP_h (Pa)	ΔP_c (Pa)	Q (W)
4	4	12,247	26,845	2,046
2.5	4	13,958	32,285	2,113
1	4	14,967	41,103	2,188

3.2 Entire length model

The entire length model is based on the same airfoil arrangement as the 4 mm (pitch X) x 4 mm (pitch Y) scaled model, but includes the total length of the PCHE (820 mm). The model is composed by a hot and a cold plate, as well as the half of the upper and lower SiC plates, where periodic boundaries have been established to simulate the succession of plates (6,000 for each fluid). The size of the mesh was about 2,900,000 elements (hexa + tetra). The inlet velocities for CO_2 and PbLi have been 3.60 m/s and 0.23 m/s, respectively. The rest of parameters were the same that in the scaled models simulations, with the exception of, in this case, k-ω with shear stress transport (SST), which is suitable for relatively low Reynolds flows, was used as turbulence model.

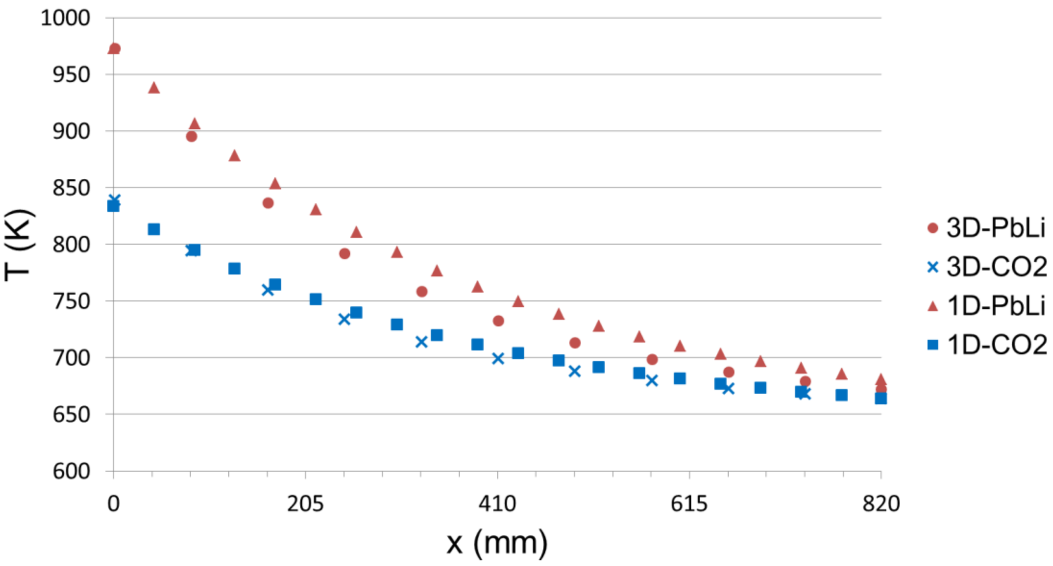

Figure 3. Temperature profiles.

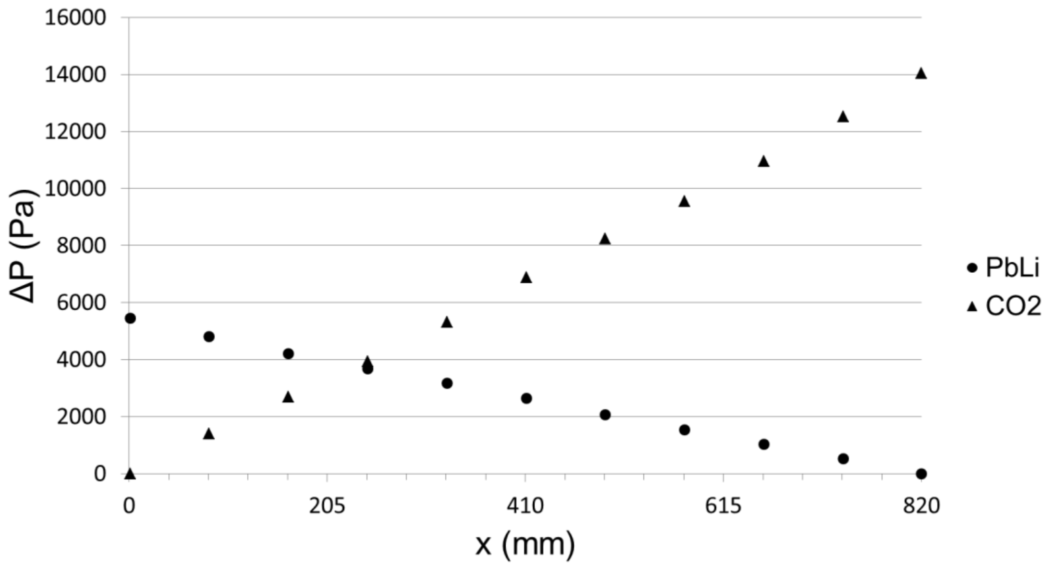

Figure 4. Pressure drops.

The above figures show close results for the temperature profiles between the 1-D and the CFD model, although the chosen empirical correlations lead to slightly underestimate the overall heat transfer coefficient. The pressure drops are low for both hot and cold streams. On the other hand, the total integrated flux of the PCHE, whose value is about 648 MW, is larger than the one expected for this heat exchanger and allows reducing the CO_2 mass flow in this sector of the Tecno_Fus power conversion layout.

4. Tritium transport model

A transport model has been developed in order to evaluate the permeation of dissolved tritium in the liquid metal breeder to the secondary CO_2.

The model has been implemented in TMAP7, a 1-D code written at Idaho National Laboratories. We suppose there is no trapping and diffusion along the direction of flow. Furthermore, only T as diffusive specimen and T_2 as enclosure specimen are considered. The solid is divided in five segments along the length of the PCHE, each of them are discretized with 5 nodes along the thickness of the plate. On the other hand, the fluid channels are divided in 10 functional enclosures (5 for PbLi and 5 for CO_2), whereas 4 boundary enclosures are disposed at the inlets and the outlets and are used as sources/sinks of tritium and volumetric flow.

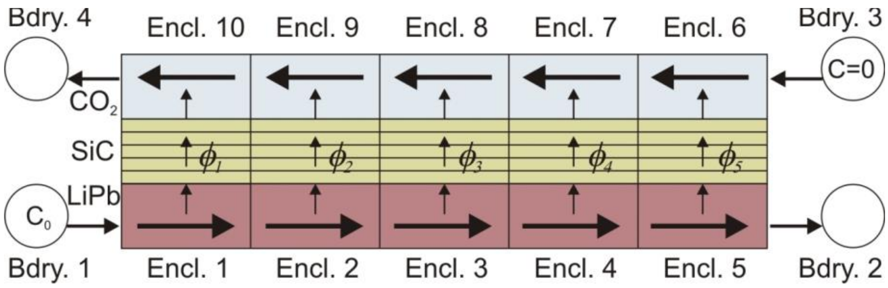

Figure 5. Process flow diagram for tritium transport.

The temperature of each functional enclosure and the segments is obtained from the CFD entire length model and fixed. The governing equations for the interfaces between enclosures and segments are the following:

$$\frac{C_{T,PbLi}}{Ks_{T,PbLi}} = \frac{C_{T,SiC}}{Ks_{T,SiC}} \quad (7)$$

$$C_{T,SiC} = Ks_{T,SiC} \cdot \sqrt{P_{T_2,CO2}} \quad (8)$$

$$J_{T,SiC} = -D_{T,SiC} \cdot \frac{\partial C}{\partial x} \quad (9)$$

Where C, Ks, P, J, D and x are concentration, Sievert's constant, partial pres6sure, flux of dissolved tritium atoms, diffusivity and normal distance to the SiC surface, respectively.

The inlet tritium concentration for the liquid metal has been calculated from [12], supposing the most unfavorable scenario without tritium extracting system before the heat exchanger.

The calculations have been made for 4 types of SiC with very different diffusivity [13] [14]. The solubility has been less widely studied, so a unique value for a β-SiC has been used for all the calculations [13]. Concentration of T in SiC and PbLi, partial pressures of T_2 in CO_2, diffusive flux to CO_2 channel and mobile inventory in SiC have been obtained.

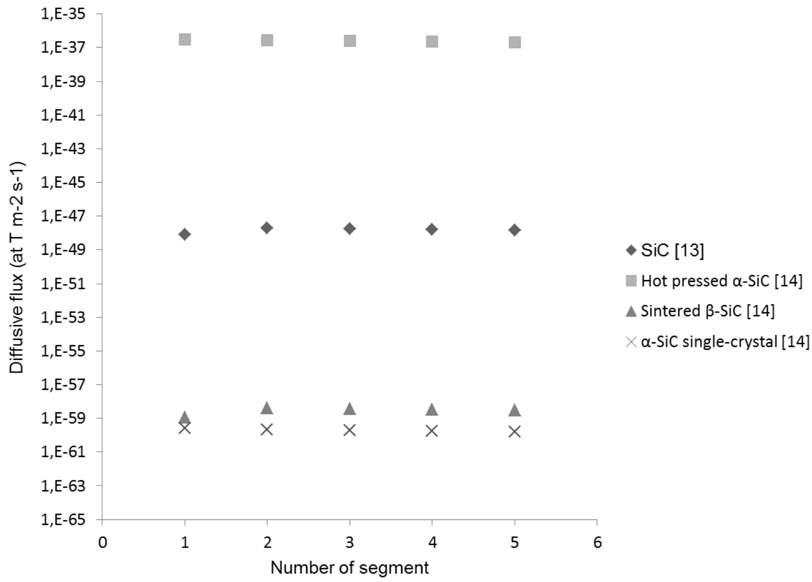

Figure 6. Diffusive flux to the CO_2 stream.

The previous figure shows the practically null diffusive flux of tritium to CO_2, whereas the final partial pressure of T_2 in the secondary is lower than the tolerance of the code, which demonstrates the efficacy of silicon carbide as tritium permeation barrier.

5. Conclusions

A design for a lithium-lead/supercritical CO_2 printed circuit heat exchanger which optimizes the pressure drop performance has been studied, and the equipment has been pre-sized for its use in a DCLL power conversion cycle. Together with the use of silicon carbide as structural material, whose efficiency as tritium permeation barrier has been demonstrated, it supposes an interesting research line to be developed.

References

[1] J. I. Linares et al., Fus. Eng. and Des. 86, 2735-2738 (2011).
[2] J-E Cha et al., KAERI report TR-3680/2008.
[3] B. Riccardi et al., J. of Nuc. Mat. 329-333 (2004), 56-65.
[4] T. Nozawa et al., J. of Nuc. Mat. 386-388 (2009), 622-627.
[5] L. L. Snead et al., J. of Nuc. Mat. 417 (2011), 330-339.
[6] Y. Takeuchi et al., Fus. Eng. and Des. 85 (2010), 1266-1270.
[7] A. V. Zinovev et al., Ceramic Engineering & Science Proceedings, volume 25 (2004), 405-410.
[8] H. Song, "Investigations of a printed circuit heat exchanger for supercritical CO_2 and water", Kansas State University (2007).
[9] E. Mas de les Valls, J. of Nuc. Mat. 376 (2008), 353-357.
[10] NIST database (http://webbook.nist.gov/chemistry/fluid/)
[11] Y-H Park et al., J. of Nuc. Mat. 386-388 (2009), 1014-1017.
[12] I. Palermo et al., Fus. Eng. and Des. 87 (2012), 1019-1024.
[13] R. A. Caussey et al., J. of Nuc. Mat. 203 (1993), 196-205.
[14] G. A. Esteban et al., J. of Nuc. Mat. 307-311 (2002), 1430-1435.